Velocity Fluctuations in a Slowly Sheared Bubble Raft

Michael Dennin

Department of Physics and Astronomy, University of California at Irvine, Irvine, California 92697-4575
(Dated: February 2, 2008)

A surprising feature of flow in slowly sheared model foam (bubble raft) is a measured discontinuity in the rate of strain as a function of position such that part of the system is "flowing" and the rest is undergoing "elastic" deformations [J. Lauridsen, G. Chanan, and M. Dennin, Phys. Rev. Lett. **93**, 018303 (2004)]. Detailed measurements of the distribution of nonlinear bubble rearrangements have been reported in connection with this discontinuity. In this paper, measurements of the fluctuations in velocity under the same conditions are reported. The fluctuations are characterized by the second and third moments of the velocity distribution. A surprising feature is the qualitative behavior of these moments as a function of position in the system, especially across the discontinuity in rate of strain. In addition, the measured dependence of the second moment of the velocity fluctuations on rate of strain is compared with predictions of simulations of the bubble model and reasonable agreement is found.

I. INTRODUCTION

Bubble rafts (single layers of bubbles floating on a water surface) serve as a model two-dimensional foam [1, 2]. When subjected to sufficiently slow rates of strain, a bubble raft exhibits an interesting discontinuity in the rate of strain ($\dot{\gamma}$) as a function of position [3]. Similar discontinuities in $\dot{\gamma}$ have been observed for high rates of strain in a number of other complex fluids [4, 5]. This is in contrast to cases of flow localization in which the rate of strain is continuous, as has been observed in granular systems [6, 7, 8] and confined two-dimensional foams [9]. The discontinuity of strain rate in bubble rafts was observed for flow between two concentric cylinders (Couette flow). At a critical radius (r_c), the system is divided into a "flowing" region for $r < r_c$ and a region undergoing "elastic" deformations for $r > r_c$. Because of the concentric cylinder geometry, the immediate question raised by the measurements in Ref. [3] is the connection between the discontinuity in $\dot{\gamma}$ and the yield stress of the bubble raft. For both general foams and the bubble raft, the yield stress is the critical stress below which flow does not occur and the system acts as an elastic solid [10, 11]. Simple arguments suggest that the existence of coexistence between flow and elastic behavior is not surprising under the geometry used in Ref. [3]. However, the same arguments suggest that the rate of strain should be continuous across the transition. The arguments depend on the combination of a yield stress for the fluid and a spatially varying stress field due to the Couette geometry [12].

In the Couette geometry, the stress decreases as a function of radial distance away from the inner cylinder [12]. Therefore, for a yield stress fluid sheared in a Couette geometry, one expects a region of flow close to the inner cylinder and, if the stress drops below the yield stress, a critical radius above which the system does not flow. Even for a yield stress fluid, it is generally expected that the stress is a *continuous* function of the rate of strain (e.g. Bingham plastic or Herschel-Bulkley models of yield stress fluids [12]). Therefore, one expects the *rate of strain* to be continuous across the transition from flow to no flow. This is what makes the observation of a discontinuity in rate of strain as a function of position so surprising.

The discontinuity in the rate of strain was determined from measurements of the average velocity of the bubbles as a function of radial position [3]. It is interesting to ask how the fluctuations in velocity behave near this discontinuity, and whether or not the radial dependence of the velocity fluctuations can shed any light on the source of the discontinuity. The velocity fluctuations are interesting for another reason. In granular systems, one often defines a "granular temperature" in terms of the root mean squared value of the velocity. In this context, there have been a number of studies of the dependence of velocity fluctuations in a variety of granular flows [13, 14, 15, 16]. It is interesting to ask if similar ideas carry over to foam, and such a study has been done using simulations of the bubble model for foam [17].

The bubble model is a simplified description of foam that has been successful in capturing a number of observed features in bubble rafts and other foam systems [18, 19, 20]. The bubble model treats foam as a collection of spherical bubbles. There are only two forces in the bubble model that act on the bubbles. The distortion of bubbles upon contact is accounted for by a repulsive spring force proportional to the degree of overlap. Dissipation within the foam is accounted for by including a viscous force proportional to the velocity difference between two bubbles. These two forces are balanced to determine the dynamics of the individual bubbles. Using the bubble model, a detailed study of velocity fluctuations as a function of packing fraction and applied rate of strain was reported on in Ref. [17]. One main result is the dependence of the second moment of velocity fluctuations on rate of strain. It was found that the second moment followed a power law as a function of rate of strain for all values of rate of strain studied. This contrasted with a range of alternate definitions of effective temperature, for which a constant value of effective temperature was reached for sufficiently low rate of strain

[17, 21]. Also of interest to the work presented here is the fact that non-Gaussian tails in the velocity distribution were measured for sufficiently slow rates of strain.

In this paper, the velocity fluctuations for a bubble raft under conditions of constant rate of strain in a Couette geometry are reported. As discussed, under these conditions, there are two regimes. Initially, the system acts as an elastic material. Above a critical strain value, plastic flow occurs. The plastic flow is characterized by irregular periods of stress increase and decrease, with a constant average value of the stress [10, 11, 22]. It is during plastic flow that a discontinuity in rate of strain as a function of radial position in the system was observed [3]. In this paper, the second and third moments of the velocity distributions are considered. A number of results are discussed. First, for low rates of strain, the second moment of the velocity distribution monotonically decreases with decreasing rate of strain. Second, during flow, there is a clear asymmetry in the velocity distribution that is apparent in measurements of the third moment. Finally, comparison is made between the velocity fluctuations during the initial elastic deformation and in the zero rate of strain region during flow.

II. EXPERIMENTAL METHODS

The experimental system has been previously described in some detail [23]. It consisted of a standard bubble raft [1, 2] in a Couette geometry (two concentric cylinders with a fluid confined in the region between the cylinders). For the experiments discussed here, the outer radius was fixed at $r_o = 7.43$ cm. The inner barrier, or rotor, is a Teflon disk with a radius $r_i = 3.84$ cm. The outer edge of the disk is a knife edge that is just in contact with the water surface. It was suspended by a wire to form a torsion pendulum. The bubble raft was produced by flowing regulated nitrogen gas through a hypodermic needle into a homogeneous solution of of 80% by volume deionized water, 15% by volume glycerine, and 5.0% by volume Miracle Bubbles (Imperial Toy Corp.). The bubble size was dependent on the nitrogen flow rate, which was varied using a needle valve. A random distribution of bubble sizes was used, with an average radius of 1 mm. The resulting bubbles were spooned into a cylindrical Couette viscometer. This produced a two-dimensional model of a wet foam on a homogeneous liquid substrate.

An important feature of the bubble raft is the gas area fraction. To achieve a desired gas area fraction, the bubble raft was constructed by placing the approximate number of desired bubbles in the trough with the outer barrier set to a large radius. It is important to note that the bubbles exhibited a strong attraction to each other. The outer barrier was compressed until the desired radius was reached. The gas area fraction was determined by thresholding images of the bubbles and counting the area inside of the bubbles. Because of the three-dimensional nature of the bubbles, this represents an operational definition

of gas-area fraction based on the details of the image analysis. However, it is also consistent with an estimate of the gas area fraction based on the area of trough and expected distribution of bubble sizes. For all of the data reported here, the gas area fraction was approximately 0.95.

Flow is generated in the bubble raft by rotating the outer Teflon barrier at a constant angular velocity. Results for two angular velocities are reported: $\Omega = 8 \times 10^{-4}$ rad/s and $\Omega = 5 \times 10^{-3}$ rad/s. The first layer of bubbles at either boundary did not slip relative to the boundary. Due to the finite size of the bubbles, this results in an effective inner radius of $r = 4.4$ cm. Due to the cylindrical geometry, the rate of strain is not uniform across the system and is given by $\dot{\gamma} = r \frac{d}{dr} \frac{v(r)}{r}$. Here $v(r)$ is the azimuthal velocity of the bubbles. This allows for studies of the velocity fluctuations over a wide range of rates of strain, even though only two different rotation rates were used.

The details of the velocity measurements are given in Ref [3]. Video images of roughly one third of the trough were recorded and individual bubbles motions were tracked. The system is divided into equally spaced radially bins. Two different types of radial bins are used. First, to compute the rate of strain, bins of equal radial spacing are used. Second, to compute properties as a function of the rate of strain, bins of equal strain rate are used. Within each bin, the bubble tracks are used to compute the average velocity, second moment of the velocity distribution $< (v - \bar{v})^2 >$, and the third moment of the velocity distribution $< (v - \bar{v})^3 >$ for the bin of interest. In these expressions, the braces refer to an average over all bubbles, and $\bar{v}$ is the mean velocity for the bin of interest. For purposes of comparing with simulations, the variance ($\delta v = \sqrt{< (v - \bar{v})^2 >}$) is considered, as well.

Before presenting the new results on the fluctuations, it is useful to repeat what is already known from Ref. [3]. First, for $\Omega = 8 \times 10^{-4}$ rad/s, the critical radius at which the rate of strain discontinuity occurs is $r_c = 6.7$ cm. For $\Omega = 5 \times 10^{-3}$ rad/s, $r_c = 6.3$ cm. For this paper, the region $r < r_c$ will be referred to as the *flowing region*, and the region with $r > r_c$ will be referred to as the *elastic deformation region*. This is distinct from the difference between the *initial elastic response* and the *steady-state flow*, which refer to distinct time periods under steady strain. The rates of strains used in this paper are taken from the same fits reported in Ref. [3]. The velocity data is fit in the region where flow occurs, assuming a power law dependence of the velocity. This fit is then used to determine the rate of strain by analytically taking the derivative.

III. EXPERIMENTAL RESULTS

Figure 1 shows the results for $\delta v = \sqrt{< (v - \bar{v})^2 >}$ as a function of shear rate. Both data from $\Omega = 8 \times 10^{-4}$ rad/s

and $\Omega = 5 \times 10^{-3}$ rad/s are shown. As a guide to the eye, the solid line represents the curve $\delta v = 0.059 x^{0.55}$. A number of features of the behavior of δv are worth noting.

First, the general trend for low rates of strain is consistent with the simulations of the bubble model [17]. Even the exponent for the power law behavior is in reasonable agreement. Assuming $\delta v \propto x^n$, the experimental data is consistent with $n = 0.55 \pm 0.05$. The simulations give $n = 0.6$. The surprising feature is the decrease in δv for rates of strain above approximately 0.02 s^{-1}. This is a feature that is not reported in regard to the simulations.
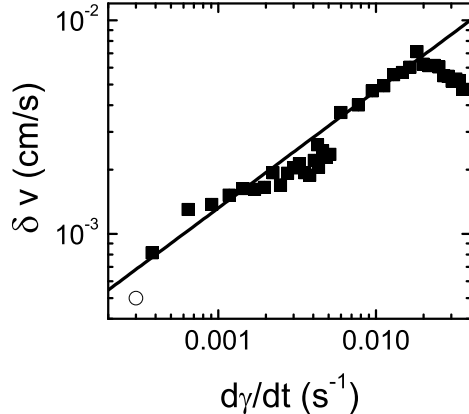

FIG. 2: A plot of the second moment ($< (v - \bar{v})^2 >$) of the velocity distribution versus radial position in the system (left hand axis), and a plot of third moment ($< (v - \bar{v})^3 >$) of the velocity distribution versus radial position in the system (right hand axis). All of the data is for $\Omega = 5 \times 10^{-3}$ rad/s. The open squares (second moment) and down triangles (third moment) are during flow, and the solid squares (second moment) and open circles (third moment) are during the initial elastic deformation. The vertical line indicates the radial position of the rate of strain discontinuity.

FIG. 1: A log-log plot of the variance ($\delta v = \sqrt{< (v - \bar{v})^2 >}$) as a function of rate of strain. The squares are data taken from the flowing regime, and the open circle is data taken from the initial elastic regime. The solid line is the curve $\delta v = 0.59 x^{0.55}$. At a rate of strain of 0.02 s^{-1}, there is a maximum in the variance. For higher rates of strain, the variance decreases.

Figures 2 and 3 illustrate the general behavior of the second and third moment of the system as a function of radial position for the two rotation rates studied: $\Omega = 5 \times 10^{-3}$ rad/s and $\Omega = 8 \times 10^{-4}$ rad/s, respectively. For comparison, the data for the initial elastic deformation is included in each plot. This data sets a baseline expectation for the measurements of fluctuations. The main source of fluctuations during the flow is expected to be nonlinear, neighbor switching events known as T1 events. These are rearrangements of bubbles in which bubbles exchange neighbors. During the initial elastic flow, there are no observed T1 events [24]. However, because of the method used to measure stress, there is motion of the inner barrier. This results in a small, non-zero rate of strain near the inner boundary during the initial elastic flow [24]. Various factors besides the T1 events contribute to velocity fluctuations during this period, such as effects due to the finite size of the bubbles and experimental noise. For comparison to the fluctuations during flow, the open circle in Fig. 1 is the value for δv during this initial elastic period.

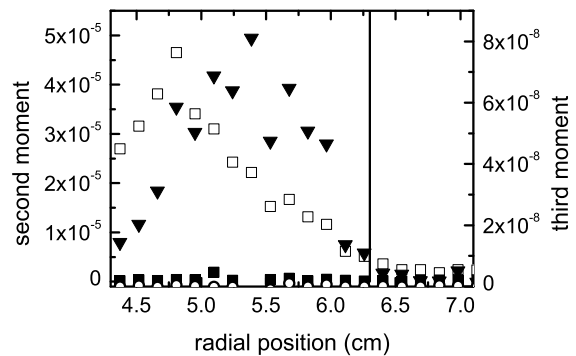A number of features of the fluctuations are evident from the plots in Figs. 2 and 3. First, recalling that $\dot{\gamma}$ decreases as the radius increases for Couette flow, the $\dot{\gamma}$ dependence of the second moment is apparent in Figs. 2 and 3. Second, there is no obvious discontinuity in the second moment at r_c. For $\Omega = 5 \times 10^{-3}$ rad/s, even in the elastic deformation region, the second moment during flow is always significantly larger than the second moment during the initial elastic response. Finally, there is a dramatic increase in the third moment in the flowing region. This indicates the development of an asymmetry in the velocity distribution.

The development of an asymmetry in the velocity distribution is illustrated in Fig. 4. Here the velocity distribution is plotted for two different radial positions with $\Omega = 8 \times 10^{-4}$ rad/s. The solid bars are for $r = 4.52$ cm, and the open bars are for $r = 6.98$ cm. In fact, one can see both the shift in average velocity and change in the second moment, as well as the development of an asymmetric distribution, for increasing $\dot{\gamma}$ (decreasing r).

Another feature of the distribution that is worth mentioning is the observation of non-Gaussian tails. This is illustrated in Fig. 5. Here a typical probability distribution for the difference in azimuthal velocity from the mean is plotted. The case shown here is for a rate of strain of 1.1×10^{-3} s^{-1}. For comparison with Ref. [17], the data is normalized by the variance, δv, so the probability distribution for $\Delta v = (v - \bar{v})/\delta v$ is considered. Also for comparison, a Gaussian distribution is included in the plot. The use of a semi-log scale highlights the non-Gaussian tails of the distribution.
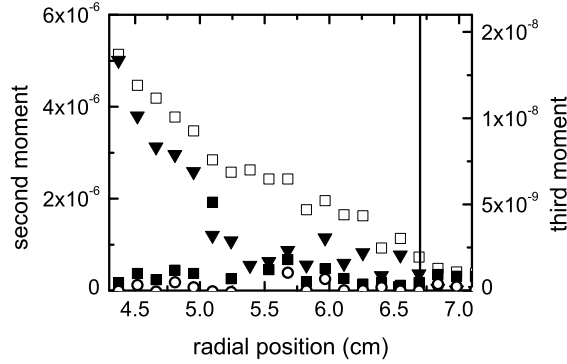
FIG. 3: A plot of the second moment ($< (v - \bar{v})^2 >$) of the velocity distribution versus radial position in the system (left hand axis), and a plot of third moment ($< (v - \bar{v})^3 >$) of the velocity distribution versus radial position in the system (right hand axis). All of the data is for $\Omega = 8 \times 10^{-4}$ rad/s. The open squares (second moment) and down triangles (third moment) are during flow, and the solid squares (second moment) and open circles (third moment) are during the initial elastic deformation. The vertical line indicates the radial position of the rate of strain discontinuity.

FIG. 5: Comparison of the probability distribution of $\Delta v = (v - \bar{v})/\delta v$ for a rate of strain of 1.1×10^{-3} s^{-1} (solid squares) with a Gaussian distribution (solid line). The data was taken at $r = 5.8$ cm with $\Omega = 8 \times 10^{-4}$ rad/s. The semi-log plot highlights the non-Gaussian tails in the experimental distribution.
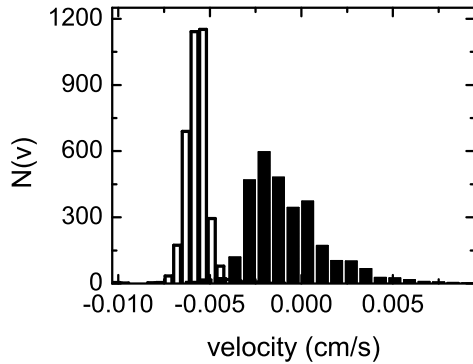

FIG. 4: Distributions of velocities for $\Omega = 8 \times 10^{-4}$ rad/s. The two distributions are taken at different radial positions. The open bars are for $r = 6.98$ cm, and solid bars are for $r = 4.52$ cm. The two distributions were selected to illustrate the evolution of an asymmetry in the velocity distributions during flow.

IV. DISCUSSION

The bubble model has been successful at explaining many features of slowly sheared bubble rafts, especially in relation to the fluctuations in stress as the bubble raft flows [22, 25]. One feature of the bubble raft flow that is not immediately obvious from the bubble model simulations is the existence of the discontinuity in rate of strain [3]. The measurements of velocity fluctuations presented here further explore this discontinuity and various predictions of the bubble model.

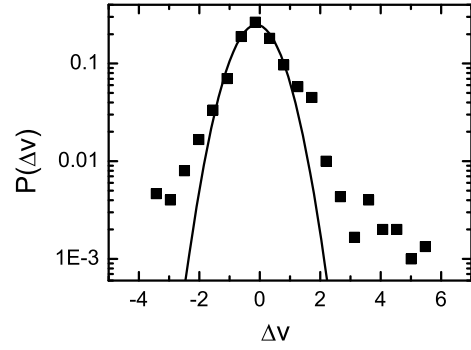There is basic agreement between the experimental measurements of the second moment of the velocity fluc-

tuations and the bubble model. In both cases, the root mean squared fluctuations are consistent with a power-law dependence on the rate of strain for low rates of strain with an exponent of approximately 0.6 [17]. The quantitative agreement is intriguing because there was no attempt to match detailed features of the system to the model, such as the dissipation or packing fraction. This agreement raises the question of how robust this exponent is, and what features of the system determine its value. Even further, this exponent is in general agreement with similar measurements in granular flow [13, 14, 15, 16], providing further support for a potential generalized description of these systems in terms of a jamming transition [26, 27]

A clear disagreement between the bubble model and the experiments is the behavior of the second moment at high rates of strain. For the experiments, the second moment of the velocity distribution appears to decrease above a rate of strain of approximately 0.02 s^{-1}. In contrast, the simulations observe a monotonic increase in the second moment as a function of increasing rate of strain to rates of strain of order 1 [17].

The sudden decrease in the second moment with rate of strain raises two issues. First, it should be noted that in the experiments, the decrease occurs at approximately the same rate of strain for which it has been reported that the system makes the transition to quasi-static behavior where the average stress is essentially independent of rate of strain. In Ref. [25], this was reported to occur at a rate of strain of 0.07 s^{-1}. However, the transition to quasi-static flow is not a sharp transition, and a gap in the data in that work from 0.01 s$^{-1} < \dot{\gamma} < 0.08$ s^{-1} makes determining its location difficult. Second, from Fig. 2, it is clear that the region of large rate of strain is also a region relatively close to one of the system's boundaries. This raises the issue of the impact of the boundaries on fluctuations. Further work with larger systems will be

needed to resolve the role of boundaries.

The other clear agreement between the bubble model and the experiments is the existence of non-Gaussian tails in the velocity distribution [17]. However, a result that needs to be explored further is the asymmetry of the velocity distribution. This asymmetry has not been reported for simulations of the bubble model. However, the simulations did focus on the equivalent of the radial velocity. In the experiments, the radial velocity was too small for accurate measurements of the velocity distribution. Therefore, before definite conclusions can be drawn, it is necessary to consider the distribution for the velocity in the direction of flow within the context of the bubble model. Besides differences between velocities parallel and perpendicular to the flow, the experiment and simulations use different geometries. It may be that the asymmetry is a result of the Couette geometry, and it does not exist in a parallel plate geometry. Future experiments are planned for the parallel plate geometry that will help resolve this issue.

Finally, the behavior near the discontinuity in strain rate raises some interesting issues. Measurements of the average rate of strain suggest that for $r > r_c$, the system is acting as an elastic solid and that there is a discontinuity in the rate of strain at r_c. However, measurements of the velocity fluctuations clearly indicate a difference between the deformation for $r > r_c$ during flow and the "real" elastic deformation observed during the initial stages of rotation. First, there is no obvious discontinuity in either the second or third moment of the velocity distribution. Second, especially for $\Omega = 5 \times 10^{-3}$ rad/s, the second and third moments of the velocity distribution, though essentially constant for $r > r_c$, are significantly larger than the values observed during the initial elastic rise. This indicates significant non-elastic motion of the bubbles in this region. These results are consistent with previous observations of nonlinear rearrangements, or T1 events. In Ref. [24], it was found that the T1 events occur at all radii, even though the flow is localized to $r < r_c$. This confirms the non-elastic nature of bubble motions during flow in the region $r > r_c$. Again, future work on larger systems will be needed to further increase our understanding of this interesting discontinuity and to better understand the nature of the zero rate of strain state for $r > r_c$ during flow.

V. ACKNOWLEDGMENTS

[1] L. Bragg and W. M. Lomer, Proc. R. Soc. London, Ser. A **196**, 171 (1949).
[2] A. S. Argon and H. Y. Kuo, Mat. Sci. and Eng. **39**, 101 (1979).
[3] J. Lauridsen, G. Chanan, and M. Dennin, Phys. Rev. Lett. **93**, 018303 (2004).
[4] P. Coussot, J. S. Raynaud, F. Bertrand, P. Moucheront, J. P. Guilbaud, and H. T. Huynh, Phys. Rev. Lett. **88**, 218301 (2002).
[5] F. D. Cruz, F. Chevoir, D. Bonn, and P. Coussot, Phys. Rev. E **66**, 051305 (2002).
[6] D. Howell, R. P. Behringer, and C. Veje, Phys. Rev. Lett. **82**, 5241 (1999).
[7] D. M. Mueth, G. F. Debregeas, G. S. Karczmar, P. J. Eng, S. R. Nagel, and H. M. Jaeger, Nature **406**, 385 (2000).
[8] W. Losert, L. Bocquet, T. C. Lubensky, and J. P. Gollub, Phys. Rev. Lett. **85**, 1428 (2000).
[9] G. Debrégeas, H. Tabuteau, and J. M. di Meglio, Phys. Rev. Lett. **87**, 178305 (2001).
[10] A. M. Kraynik, Ann. Rev. Fluid Mech. **20**, 325 (1988).
[11] D. Weaire and S. Hutzler, *The Physics of Foams* (Claredon Press, Oxford, 1999).
[12] R. B. Bird, R. C. Armstrong, and O. Hassuage, *Dynamics of Polymer Liquids* (Wiley, New York, 1977).
[13] N. Menon and D. J. Durian, Science **275**, 1920 (1997).
[14] W. Losert, D. G. W. Cooper, J. Delour, A. Kudrolli, and J. P. Gollub, Chaos **9**, 682 (1999).
[15] P. A. Lemieux and D. J. Durian, Phys. Rev. Lett. **85**, 4273 (2000).
[16] D. Mueth, Phys. Rev. E **67**, 011304 (2003).
[17] I. K. Ono, S. Tewari, S. A. Langer, and A. J. Liu, Phys. Rev. E **67**, 061503 (2003).
[18] D. J. Durian, Phys. Rev. Lett. **75**, 4780 (1995).
[19] D. J. Durian, Phys. Rev. E **55**, 1739 (1997).
[20] S. Tewari, D. Schiemann, D. J. Durian, C. M. Knobler, S. A. Langer, and A. J. Liu, Phys. Rev. E **60**, 4385 (1999).
[21] I. K. Ono, C. S. O'Hern, D. J. Durian, S. A. Langer, A. J. Liu, and S. R. Nagel, Phys. Rev. Lett. **89**, 095703 (2002).
[22] J. Lauridsen, M. Twardos, and M. Dennin, Phys. Rev. Lett. **89**, 098303 (2002).
[23] R. S. Ghaskadvi and M. Dennin, Rev. Sci. Instr. **69**, 3568 (1998).
[24] M. Dennin, Phys. Rev. E p. in press (2004).
[25] E. Pratt and M. Dennin, Phys. Rev. E **67**, 051402 (2003).
[26] A. J. Liu and S. R. Nagel, Nature **396**, 21 (1998).
[27] A. J. Liu and S. R. Nagel, eds., *Jamming and Rheology* (Taylor and Francis Group, 2001).